RSC Advances

PAPER

View Article Online
View Journal | View Issue

Cite this: *RSC Adv.*, 2020, **10**, 28193

Palladium nanoparticles-anchored dual-responsive SBA-15-PNIPAM/PMAA nanoreactor: a novel heterogeneous catalyst for a green Suzuki–Miyaura cross-coupling reaction†

Anandhu Mohan,[a] Lipeeka Rout,[a] Anju Maria Thomas,[a] Jerome Peter,[a] Saravanan Nagappan,[a] Surendran Parambadath[b] and Chang-Sik Ha *[a]

To develop a sustainable and cost-effective catalyst for cross-coupling reactions, dual (temperature and pH)-responsive poly(*N*-isopropyl acrylamide-*co*-methacrylic acid) (PNIPAM/PMAA) functionalised SBA-15 was synthesised *via* free radical polymerisation using potassium persulfate as an initiator and decorated with palladium nanoparticles (PdNPs-SBA-15-PNIPAM/PMAA). The X-ray photoelectron spectroscopic analysis revealed that the Pd content in the zero oxidation state of the catalyst was 1.21 wt%. The dynamic light scattering studies showed that the catalyst exhibited swelling behaviours at low temperatures (<32 °C) and high pH (>4), but exhibited deswelling behaviours at high temperatures (>32 °C) and low pH (<4). To examine the performance of the catalyst, Suzuki–Miyaura cross-coupling (SMC) reaction was conducted under batch reaction conditions. The reaction conditions were optimised with various parameters using phenylboronic acid and bromobenzene as the model substrates. High conversions (>90%) were realized for the room-temperature SMC reaction in an aqueous medium for various substituted aryl halides, while the conversion was low at relatively high temperatures (>32 °C). The conversion was dependent on the different electronic effects between the electron-releasing and electron-withdrawing groups of the aryl halides. After the experiment, the catalyst was successfully recovered without any loss of heterogeneity and could be reused at least up to the fifth cycle.

Received 10th June 2020
Accepted 22nd July 2020

DOI: 10.1039/d0ra05786j

rsc.li/rsc-advances

Introduction

Recently, the formation of carbon–carbon (C–C) bonds using various named reactions has attracted substantial attention. Among various reactions for C–C bond formation, the Suzuki–Miyaura cross-coupling (SMC) reaction, which comprises the coupling of an aryl halide and phenylboronic acid, has been known to be a more simple and efficient strategy for the preparation of biphenyls.[1,2] These synthesised biphenyls are considered important building blocks for use in various pharmaceutical and agriculture industries. Additionally, the SMC reaction of organoboronic reagents and aromatic compounds is impossible to perform in the presence of neat water because of the immiscible properties of the organic and water phases.[3,4] To rectify this issue, previous research suggests the use of phase-transfer catalysts (PTCs), which can act as a bridge between the two immiscible phases.[3,5] The addition of PTCs, such as tetrabutylammonium bromide (TBAB) and polyethylene glycol (PEG), to the immiscible mixture can form an interlayer phase boundary between these immiscible phases in the liquid mixture, and the PTC molecules can transport reactant molecules from the organic phase to aqueous phase.[3,5]

Generally, the traditional SMC reaction comprises a Pd catalyst in the presence of various ligands.[6–8] Initially, in 1981, Miyaura *et al.* proposed the use of a homogeneous Pd catalyst to perform the SMC reaction using various compounds, such as heteroaryl halides, unactivated aryl chlorides, and hindered boronic acids, under mild conditions.[9] However, there are a few drawbacks associated with these catalysts. For instance, the homogeneous form of the Pd catalysts is generally unrecyclable, and in most cases, the products formed were contaminated by residual Pd or ligands.[10,11] In addition, some ligands are generally more toxic and more expensive for large-scale applications than the noble metal itself.[11] Recently, transition metal nanoparticles are considered active catalysts for many coupling reactions owing to their high surface-to-volume ratios.[12] The co-reduction method was found to be the most common approach for the synthesis of metal nanoparticles.[2] The direct utilisation of noble metal nanoparticles in catalysis is difficult to realise

[a]*Department of Polymer Science and Engineering, Pusan National University, Busan 46241, Republic of Korea. E-mail: csha@pnu.edu*

[b]*Department of Chemistry, Government College Malappuram, University of Calicut, Kerala 676509, India*

† Electronic supplementary information (ESI) available: Wide angle XRD, Effect of catalyst amount, TEM–EDX mapping of reused catalysts and NMR spectra of the products. See DOI: 10.1039/d0ra05786j

owing to their high agglomeration behaviours resulting from van der Waals forces. To enhance the activity, prevent agglomeration behaviour, and improve the stability of this transition metal nanoparticle in the field of catalysis, a hosting or supporting material is highly recommended. Some recent studies suggest that Pd nanoparticles (PdNPs) on any form of support, such as polymers, mesoporous silicas, and metal oxides, have the potential to increase the stability and efficiency of the catalysts.[13,14]

Among various established mesoporous silicas, SBA-15 has been recognised as a potential support for transition metal nanoparticles because of their efficient activity in coupling reactions. The role of SBA-15 in such reactions has also been demonstrated in previous studies.[15,16] In addition, polymer-grafted mesoporous materials have gained significant attention in various applications.[17,18] In particular, stimuli-responsive polymeric materials have been adapted under different environmental conditions, such as temperature, pH, light, and ionic strength.[19–21] Among the various stimuli-responsive polymers, poly(methacrylic acid) (PMAA) and poly(*N*-isopropyl acrylamide) (PNIPAM) have been widely studied for different applications. PMAA is considered a pH-responsive polymer, where a change in the chain conformation occurs with a change in pH.[22] Similarly, PNIPAM changes its conformation in response to the temperature, meaning that PNIPAM chains stretch below the lower critical solution temperature (LCST) and shrink above the LCST. The coating of stimuli-responsive polymers onto the mesoporous support has gained more attention because they exhibit properties inherent to both inorganic cores and grafted polymers.[23] However, a thorough study has not been performed on the influence of the combined effect of mesoporous silica, metal nanoparticles, and grafted polymers in the coupling reaction field.

The dual stimuli-responsive behaviours, such as the temperature- and pH-responsive behaviours, in a single material can be used for multiple applications. Challengingly, we report for the first time the preparation of a novel PdNP-supported nanohybrid catalyst with temperature-responsive PNIPAM and pH-responsive PMAA. The hydrophilic ability of the catalyst at low temperatures and high pH was utilised for the SMC reaction of less activated aromatic halides at room temperature and in a water–ethanol mixture. The novelty of our new synthesised catalyst is that it can exhibit both temperature- and pH-responsive behaviours and excellent catalytic performance towards SMC reactions using an environment-friendly solvent at room temperature. Moreover, our approach is noteworthy in that a water/ethanol mixture is used as the solvent medium, and the catalytic experiment is performed at room temperature to achieve sustainability with excellent conversion. The synthesised catalyst must be valuable and preferable for industrial mass production. In addition, the PdNPs-SBA-15-PNIPAM/PMAA catalyst showed higher catalytic activity than various control catalysts. Furthermore, it exhibits relatively high or comparable catalytic activity in contrast to the catalysts in previous studies. This high performance could be attributed to the synergetic effect of the PdNPs and dual-responsive polymers. The results of the present study may assist in choosing solid catalysts and reaction parameters for the SMC reaction under mild conditions.

Experimental

Synthesis of SBA-15

SBA-15 was synthesised by a slightly modified previously reported method using Pluronic P123.[24] Typically, 16 g of P123 was mixed with 500 mL of DI water and 80 mL of concentrated HCl and stirred continuously to get a homogeneous mixture. Furthermore, the mixture was stirred in an oven at 35 °C, followed by the dropwise addition of 36.87 mL of tetraethyl orthosilicate (TEOS). The solution was stirred continuously for 1 h and kept static for another 24 h. Finally, the mixture was aged at 100 °C for approximately 24 h. Subsequently, the white solid suspension was filtered, washed with DI water/ethanol, and air-dried overnight. The P123 template was removed by calcination of the solid product at 550 °C for 8 h under air atmosphere.

Modification of SBA-15

Initially, the above-synthesised SBA-15 was pre-heated at 100 °C in a vacuum oven overnight after calcination to remove moisture. Pre-heated SBA-15 (1 g) was dispersed in 50 mL of anhydrous ethanol in a 100 mL round-bottom flask equipped with a water condenser and nitrogen balloon. This suspension was injected with 1 mL of (3-methoxysilyl) propyl methacrylate (TMSPM) and stirred for about 24 h at 60 °C. After the reaction was completed, the mixture was cooled to room temperature, and the solid particles were separated by centrifugation. The modified products were washed with ethanol, followed by drying under vacuum at 60 °C. The final product was denoted as SBA-15-TMSPM.

Synthesis of SBA-15-PNIPAM/PMAA

Firstly, SBA-15-TMSPM (0.2 g) was pre-heated at 60 °C for polymerisation and taken in a 100 mL three-necked flask. The weighed quantities of the monomers (0.35 g NIPAM and 0.15 g MAA) were taken in a 50 mL round-bottom (RB) flask and degassed separately in a 1 : 4 ethanol–water mixture (20 mL) by nitrogen purging. Furthermore, the degassed monomer solution was added to the three-necked flask containing modified SBA-15 suspensions, and it was stirred for 1 h at 80 °C under nitrogen atmosphere. Potassium persulfate (KPS) (0.02 g) was added to this mixture, and the polymerisation was continued for 4 h at 80 °C. After the suspension was cooled, the final obtained solid particles were isolated by centrifugation, followed by washing twice with DI water and ethanol. The product was denoted by SBA-15-PNIPAM/PMAA.

Incorporation of PdNPs into the SBA-15-PNIPAM/PMAA

Initially, 50 mg of SBA-15-PNIPAM/PMAA was dispersed in 10 mL of water and stirred for about 1 h. Subsequently, 0.01 M K_2PdCl_4 (dissolved in 5 mL of water) was added, and the mixture was stirred for 5 h. Thereafter, 0.1 M $NaBH_4$ (dissolved in 5 mL of water) was added dropwise to the mixture, and it was stirred

for another 2 h. The final precipitate was filtered, washed five times with water, and dried overnight under vacuum at 40 °C.

Typical procedure for the SMC reaction

The general procedure for the SMC reaction of an aryl halide with phenylboronic acid is as follows. Aryl halide (1 mmol), phenylboronic acid (1.3 mmol), K_2CO_3 (3 mmol), TBAB (0.5 mmol), PdNPs-SBA-15-PNIPAM/PMAA catalyst (3 mg), and 5 mL of a water–ethanol mixture (4 : 1 ratio) were placed in a 25 mL two necked RB flask. Subsequently, the mixture was stirred at room temperature. Aliquots were removed at one-hour intervals, and the progress of the reaction was monitored by thin-layer chromatography (TLC) and gas chromatography (GC). After the reaction was completed, the catalyst was separated by filtration, followed by washing with water and ethyl acetate (EA) (in the case of hydrophilic aryl halide, the solution is first acidified with 0.1 M HCl). The organic layer was collected, washed with water (3 × 10 mL), and dried over Na_2SO_4. Subsequently, it was concentrated by evaporation and dried over Na_2SO_4. Subsequently, it was concentrated by evaporation and dried under vacuum conditions at 35 °C. The thus-obtained product was confirmed by ^{1}H nuclear magnetic resonance (NMR) spectroscopy. The ^{1}H NMR spectral details of the products are given in ESI.†

Results and discussion

Structural characterisation of the synthesised catalyst

The PdNPs-SBA-15-PNIPAM/PMAA catalyst was synthesised by a four-step process (Scheme 1). First, we prepared the mesoporous silica SBA-15 as the base material using the sol–gel approach. Thereafter, it was modified with the vinyl coupling agent, TMSPM. In the third step, this modified SBA-15 was polymerised with NIPAM and MAA by free radical polymerisation. Finally, the PdNPs were incorporated into the polymerised SBA-15 using the co-reduction approach. The obtained PdNPs-SBA-15-PNIPAM/PMAA nanohybrid catalyst exhibited dual-responsive behaviour. The temperature-responsive property depends on the LCST of the PNIPAM moiety which exists in the hydrated state below the LCST and in the dehydrated state above the LCST.[25] The protonation and deprotonation behaviours of the carboxylic acid group in PMAA decides the pH-responsive behaviour of the catalyst. At low pH, the catalyst exists in a protonated-shrunken state, and at high pH, it exists in the deprotonated COO^- state. The electrostatic repulsion between the COO^- groups leads to the swollen structure of the catalyst.[26] The dual-responsive property of the present catalyst has been thoroughly discussed in the latter part of the discussion.

The Fourier-transform infrared (FTIR) spectra provided detailed information about the functionalisation of materials as described in the procedure. The FTIR spectra of SBA-15, SBA-15-TMSPM, and SBA-15-PNIPAM/PMAA are displayed in Fig. 1. The FTIR spectra of SBA-15 showed characteristic peaks at 805 cm^{-1} and 1090 cm^{-1} that were assigned to the in-plane bending of Si–O and Si–O–Si asymmetrical stretching vibrations, respectively. The vibrational bands at 1630 and 3440 cm^{-1} were attributed to OH bending and stretching vibrations, respectively, of the absorbed water.[27] After modifying with TMSPM, new bands at 1710 cm^{-1} and 2960–2837 cm^{-1}, attributed to the C=O stretching and C–H asymmetric and symmetric stretching vibrations of TMSPM, respectively, indicate the successful modification of SBA-15 with TMSPM. The polymerisation of MAA in SBA-15 is described by the increased intensity and slight shifting towards high wavenumbers of the peaks at 1719 cm^{-1} and 2892–2890 cm^{-1} for SBA-15-PNIPAM/PMAA.[26] In addition, the bands at 1644 cm^{-1}, 1549 cm^{-1}, and 1442 cm^{-1} were attributed to the C=O stretching vibration, N–H vibration, and

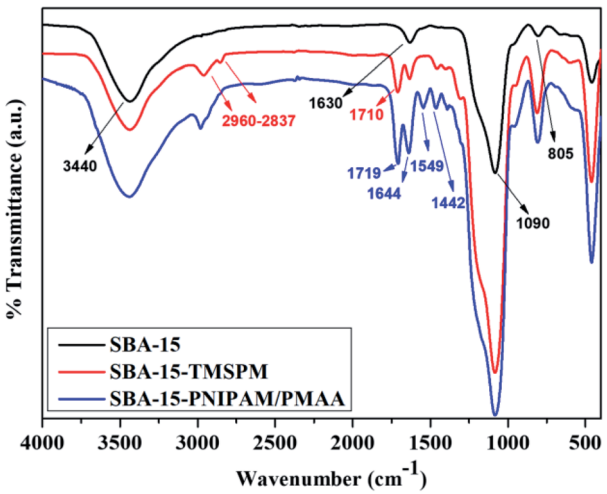

Fig. 1 FTIR spectra of SBA-15, SBA-15-TMSPM, and SBA-15-PNIPAM/PMAA.

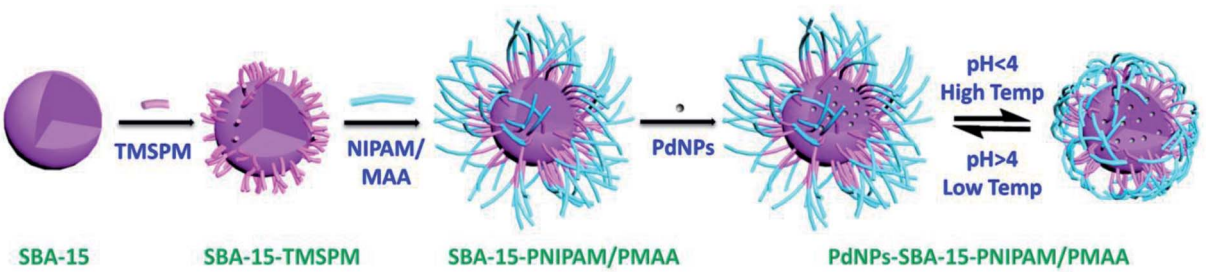

Scheme 1 Schematic representation of the synthesis of the dual-responsive PdNPs-SBA-15-PNIPAM/PMAA catalyst.

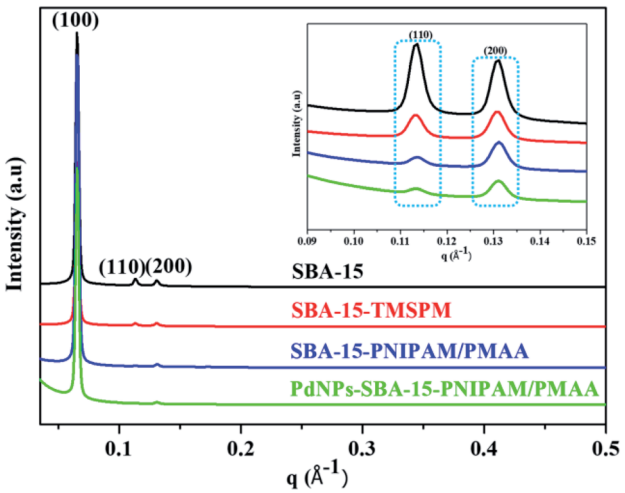

Fig. 2 SAXS patterns of SBA-15, SBA-15-TMSPM, SBA-15-PNIPAM/PMAA, and PdNPs-SBA-15-PNIPAM/PMAA.

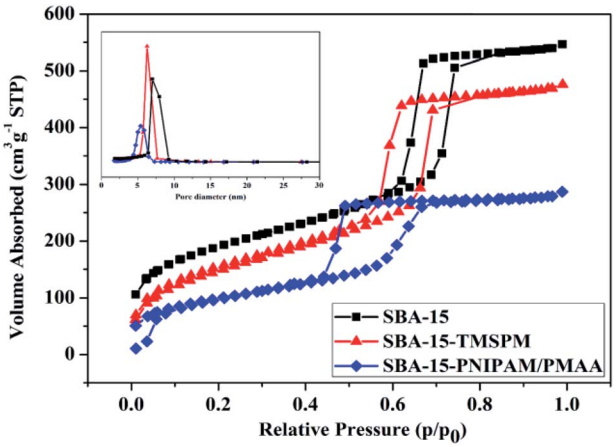

Fig. 4 Nitrogen adsorption–desorption isotherms and pore size distribution curves (inset) of SBA-15, SBA-15-TMSPM, and SBA-15-PNIPAM/PMAA.

C–H vibrations, respectively, of the temperature-responsive PNIPAM.[25] These results confirmed the successful polymerisation of MAA and NIPAM to the modified SBA-15.

The mesostructures of SBA-15, SBA-15-TMSPM, SBA-15-PNIPAM/PMAA, and PdNPs-SBA-15-PNIPAM/PMAA were studied by small-angle X-ray scattering (SAXS) analysis (Fig. 2). The SAXS patterns demonstrated typical characteristic Bragg's diffraction peaks at (100), (110), and (200), corresponding to the q values of 0.065 $Å^{-1}$, 0.11 $Å^{-1}$, and 0.13 $Å^{-1}$, respectively. After modification with the TMSPM, the intensity of the (110) and (200) peaks decreased. The existence of the three peaks after the modification demonstrates that the ordered hexagonal symmetry was maintained even after the functionalisation of the TMSPM. This further suggests the successful modification of the methacrylate group on the SBA-15 surface. The intensity of the (110) and (200) peaks decreased further after polymerisation with NIPAM and MAA. These suggest that grafting of polymer layers on the mesopore surface led to shrinkage of mesopores. The SAXS patterns proved the coating of the polymer onto SBA-15.[28] In the case of PdNPs-SBA-15-PNIPAM/PMAA, the intensity of all the three peaks decreased again, suggesting that the nanoparticles are incorporated to the mesopores of SBA-15 through the coated polymers. The wide angle X-ray diffraction (XRD) patterns of SBA-15-PNIPAM/PMAA and PdNPs-SBA-15-PNIPAM/PMAA are depicted in Fig. S1.† Unlike the SBA-15-PNIPAM/PMAA, the PdNPs-SBA-15-PNIPAM/PMAA exhibited diffraction peaks typical of PdNPs at 39°, 45°, 67°, and 80° due to the (111), (200), (220), and (311) face-centred cubic (fcc) planes of the PdNPs.[25]

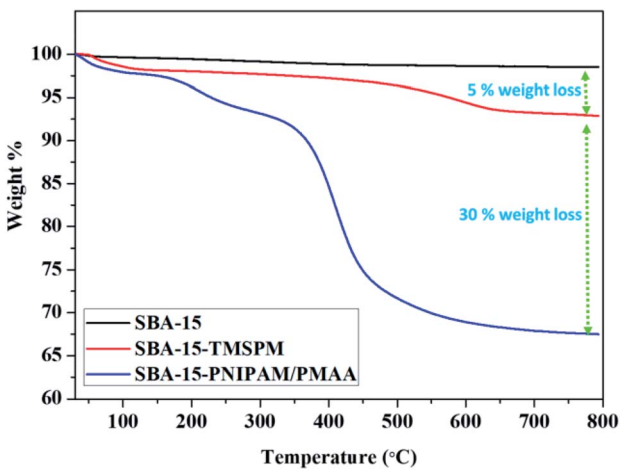

Fig. 3 TGA curves of SBA-15, SBA-15-TMSPM, and SBA-15-PNIPAM/PMAA.

The thermal stability of the synthesised samples was detected by the thermogravimetric analysis (TGA) curves. Fig. 3 shows the individual TGA curves of SBA-15, SBA-15-TMSPM, and SBA-15-PNIPAM/PMAA. The observed weight loss below 200 °C was caused by the evaporation of the physically absorbed water or solvent.[29] SBA-15 showed a weight loss of 1% due to the physisorbed water moiety and condensation of silanol groups. The weight loss of TMSPM-modified SBA-15 was found to be 5%, attributed to the decomposition of the TMSPM. After the polymerisation with PNIPAM and PMAA, the corresponding weight loss due to the decomposition of the polymers was ~30%. The TGA indicates the grafting of PNIPAM and PMAA onto SBA-15.

Nitrogen adsorption–desorption isotherm analysis was conducted to compare the mesopore structures of SBA-15, SBA-15-TMSPM, and SBA-15-PNIPAM/PMAA (Fig. 4). In all the three

Table 1 Textural properties of SBA-15, SBA-15-TMSPM, and SBA-15-PNIPAM/PMAA

Sample	Surface area (m^2 g^{-1})	Pore volume (cm^3 g^{-1})	Pore size (nm)
SBA-15	666	0.96	7.1
SBA-15-TMPSM	545	0.64	6.2
SBA-15-PNIPAM/PMAA	356	0.39	5.4

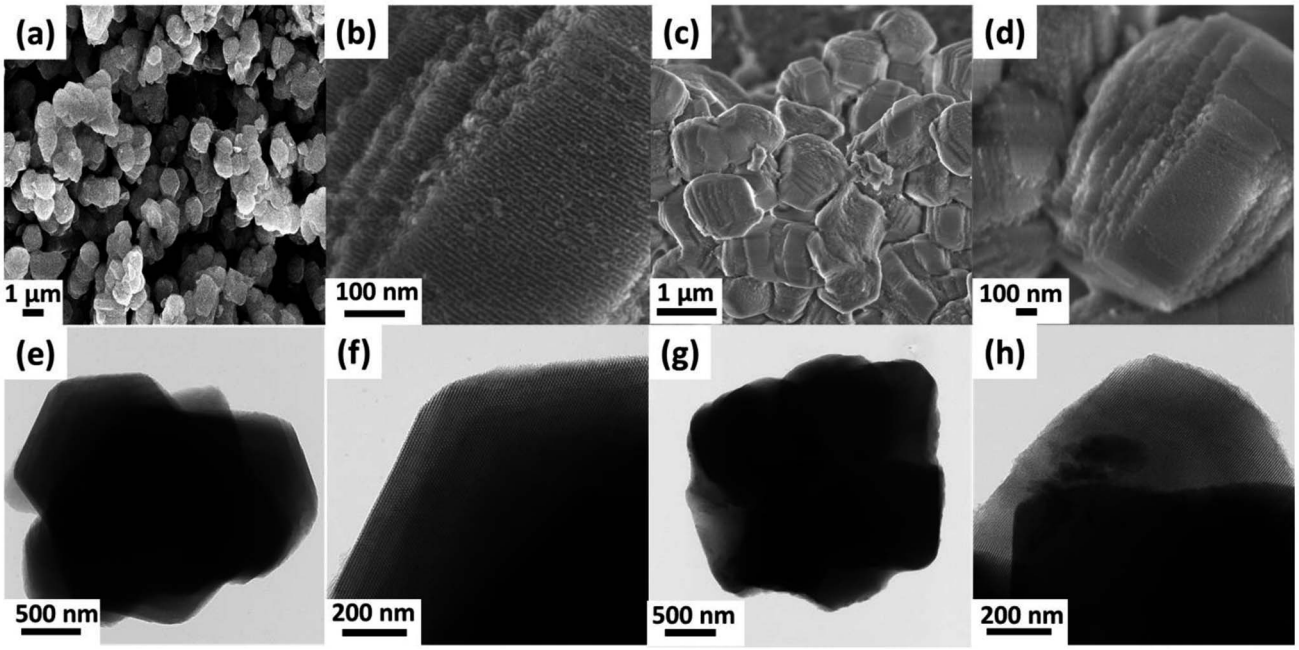

Fig. 5 FE-SEM images of SBA-15 (a and b) and PdNPs-SBA-15-PNIPAM/PMAA (c and d). FE-TEM images of SBA-15 (e and f) and PdNPs-SBA-15-PNIPAM/PMAA (g and h).

samples, we can observe a type IV isotherm with characteristic H_1 hysteresis loops in the relative pressure region between 0.4 and 0.8, which confirms that the mesoporous nature of SBA-15 was maintained even after the modification and polymerisation. The surface area calculated using the Brunauer–Emmett–Teller (BET) method was 666 $m^2\ g^{-1}$, 545 $m^2\ g^{-1}$, and 356 $m^2\ g^{-1}$ for SBA-15, SBA-15-TMSPM, and SBA-15-PNIPAM/PMAA, respectively. The cumulative pore volumes and average pore sizes calculated using the Barret–Joyner–Halenda (BJH) method were 0.96 $cm^3\ g^{-1}$ and 7.07 nm for SBA-15, 0.64 $cm^3\ g^{-1}$ and 6.2 nm for SBA-15-TMSPM, and 0.39 $cm^3\ g^{-1}$ and 5.4 nm for SBA-15-PNIPAM/PMAA, respectively (Table 1). Compared with SBA-15, the surface area, pore volume, and pore size decreased after modification and polymerisation, indicating the

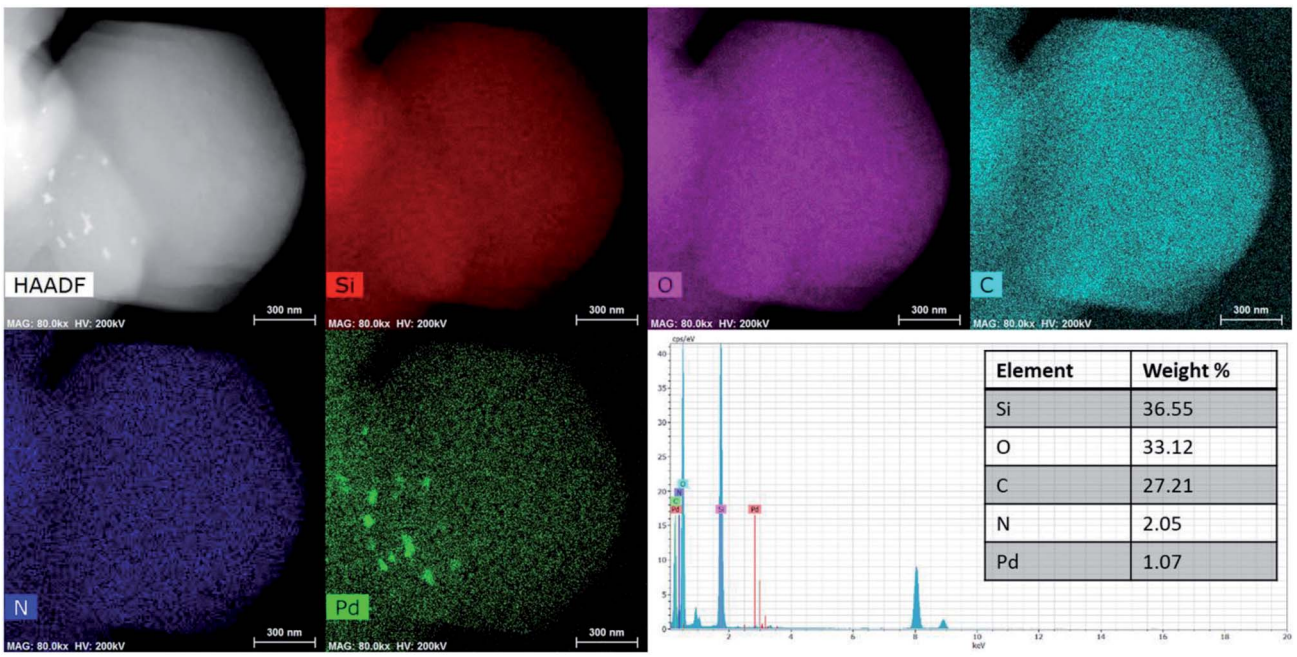

Fig. 6 HAADF-TEM and EDX mapping images of the PdNPs-SBA-15-PNIPAM/PMAA catalyst.

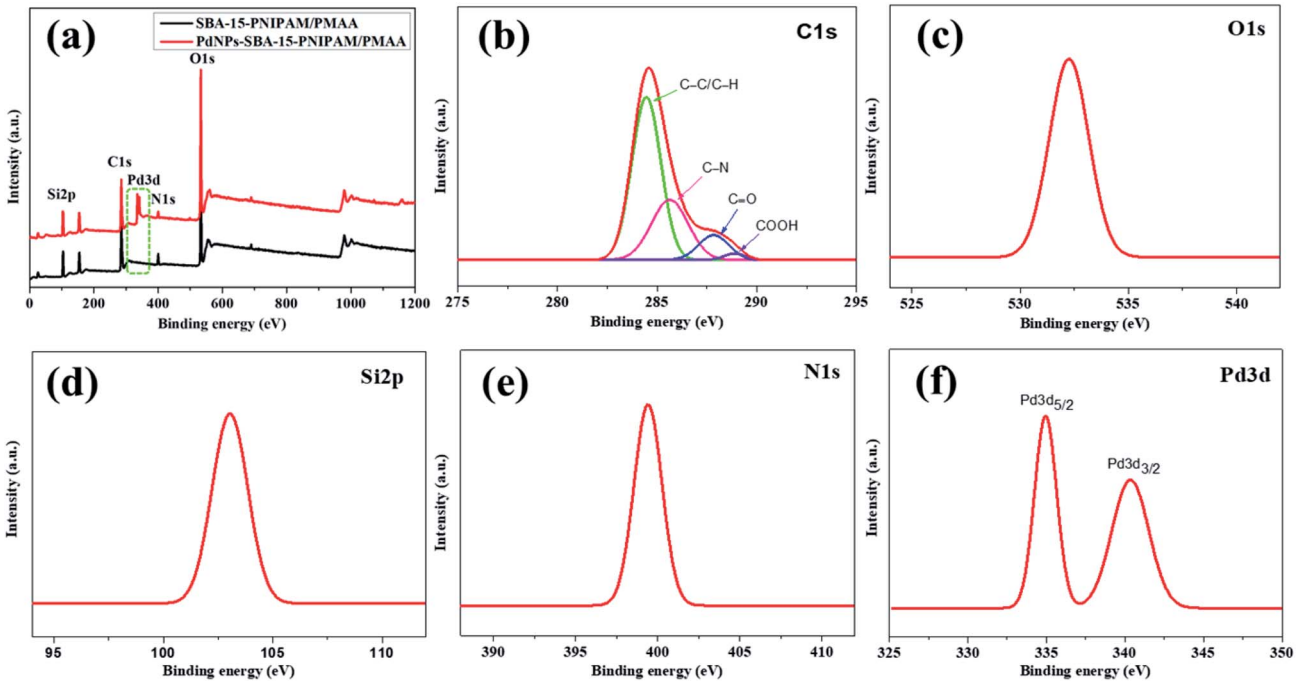

Fig. 7 (a) Survey scan spectra of SBA-15-PNIPAM/PMAA and PdNPs-SBA-15-PNIPAM/PMAA, (b) C1s XPS spectrum, (c) O1s XPS spectrum, (d) Si2p XPS spectrum, (e) N1s XPS spectrum, and (f) Pd3d XPS spectrum of the PdNPs-SBA-15-PNIPAM/PMAA catalyst.

successful modification of TMSPM and PNIPAM/PMAA on SBA-15. The reductions in pore size and pore volume demonstrated the presence of polymers both inside and outside the SBA-15 mesopore.[30]

The morphology and microstructure of the SBA-15 and PdNPs-SBA-15-PNIPAM/PMAA were studied using field-emission scanning electron microscopy (FE-SEM) and field-emission transmission electron microscopy (FE-TEM) analysis (Fig. 5). The FE-SEM images of SBA-15 (Fig. 5a and b) reveal the hexagonal block shape with a uniform particle size of 910 nm. Compared to bare SBA-15, the PdNPs-SBA-15-PNIPAM/PMAA (Fig. 5c and d) exhibits some agglomeration behaviour with a rugged surface caused by the imprinted polymer layer and PdNPs. The FE-TEM analysis was conducted to obtain information about the shape, size, and distribution details of the hybrid materials. The FE-TEM images of SBA-15 (Fig. 5e and f) confirm its uniform hexagonal pore structure, which indicates the successful formation of the SBA-15.[31] After polymerisation with PNIPAM and PMAA, the average particle size increased to 970 nm. The black dots present in the inner pore channels of the PdNPs-SBA-15-PNIPAM/PMAA are attributed to the PdNPs, which confirms the incorporation of PdNPs into the SBA-15-PNIPAM/PMAA. The average particle sizes of the PdNPs were found to be in the range 2–3 nm. The high-angle annular dark-field (HAADF)-TEM image with energy-dispersive X-ray spectroscopy (EDX) mapping reveals the uniform distribution of the PdNPs in the PdNPs-SBA-15-PNIPAM/PMAA, and the PdNP content was found to be 1.07% (Fig. 6). The EDX mapping

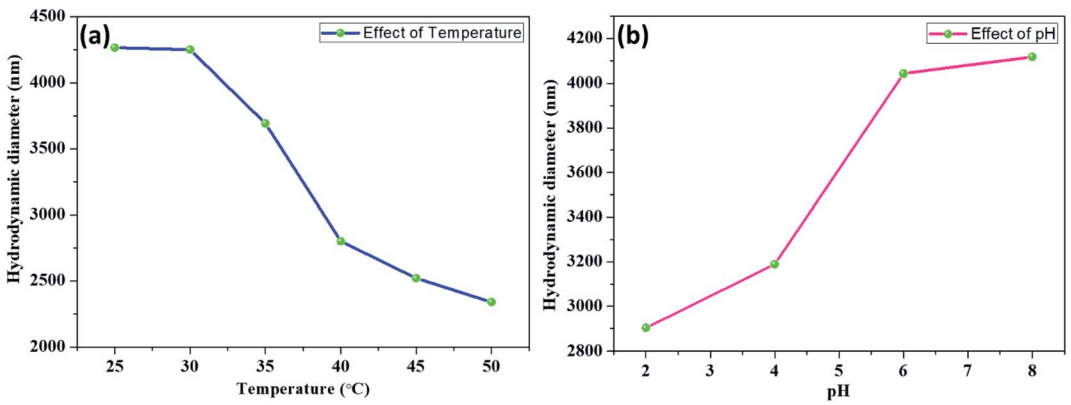

Fig. 8 Hydrodynamic diameter (D_h) of PdNPs-SBA-15-PNIPAM/PMAA as a function of various temperatures (a) at pH 6 and different pH (b) at 25 °C.

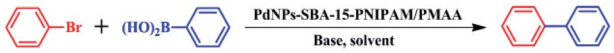

Scheme 2 The SMC reaction of aryl halides with phenylboronic acid.

also revealed the presence of other elements, such as Si, C, O, and N, which further indicates the successful polymerisation of PNIPAM and PMAA onto the SBA-15 surface.

The oxidation state and chemical composition of the PdNPs-SBA-15-PNIPAM/PMAA were examined by XPS analysis. Fig. 7a displays the survey scan spectra of SBA-15-PNIPAM/PMAA and PdNPs-SBA-15-PNIPAM/PMAA. Compared with SBA-15-PNIPAM/PMAA, an additional peak was observed in the PdNPs-SBA-15-PNIPAM/PMAA catalyst, which corresponded to the PdNPs, and this confirmed the successful incorporation of PdNPs into the catalyst. Fig. 7b shows the C1s spectrum of the PdNPs-SBA-15-PNIPAM/PMAA catalyst, where the curve is fitted into four corresponding peaks at the binding energies of 284.6 eV (C–C/C–H), 286 eV (C–N), 287.9 eV (C=O), and 289.1 eV (COOH), individually.[32] The O1s spectrum (Fig. 7c) displays the characteristic peak at the binding energy of 532.2 eV, the characteristic Si2p spectrum (Fig. 7d) at 103.1 eV, and the N1s spectrum (Fig. 7e) at 399.5 eV.[26,32] For further details on the chemical structure and oxidation state of the PdNPs, high-resolution core-level Pd3d spectra were acquired (Fig. 7f), which exhibits a doublet $Pd3d_{5/2}$ at 335 eV and $Pd3d_{3/2}$ at 340.4 eV. The energy gap between the spin-coupled core levels was 5.4 eV, which suggested that the PdNPs in the catalyst are in a zero oxidation state.[25] The composition of PdNPs from the XPS analysis was found to 1.21%, which was close to that of the which aforementioned EDX data.

The temperature- and pH-responsive behaviours of the PdNPs-SBA-15-PNIPAM/PMAA catalyst were evaluated by the changes in the hydrodynamic diameter with different temperatures and pH. Fig. 8a displays the temperature-responsive behaviour of the catalyst by a variation in hydrodynamic diameter corresponding to the temperature at pH 6. An abrupt decrease in hydrodynamic diameter was observed at temperatures between 30 and 40 °C due to the LCST phase transition behaviour of the PNIPAM moiety.[25,33] Below this temperature, the catalyst becomes hydrophilic and swells in an aqueous solution. Above the phase transition temperature, it becomes hydrophobic and shrinks in an aqueous solution. The pH-responsive behaviour of the catalyst was investigated in the pH range 2–8 at 25 °C (Fig. 8b). The DLS results show a sharp increase in the hydrodynamic diameter at pH between 4 and 6. When the pH exceeds the pKa value (pH 4), the COOH group in the methacrylic acid becomes protonated, which further creates a repulsive force between them, resulting in the swelling of catalyst.[26,34] These results highlight the dual-responsive behaviour of the PdNPs-SBA-15-PNIPAM/PMAA catalyst.

Catalytic activity

As described in Scheme 2, the catalytic activity of the synthesised dual-responsive PdNPs-SBA-15-PNIPAM/PMAA catalyst towards the SMC reaction of aryl halides and phenylboronic

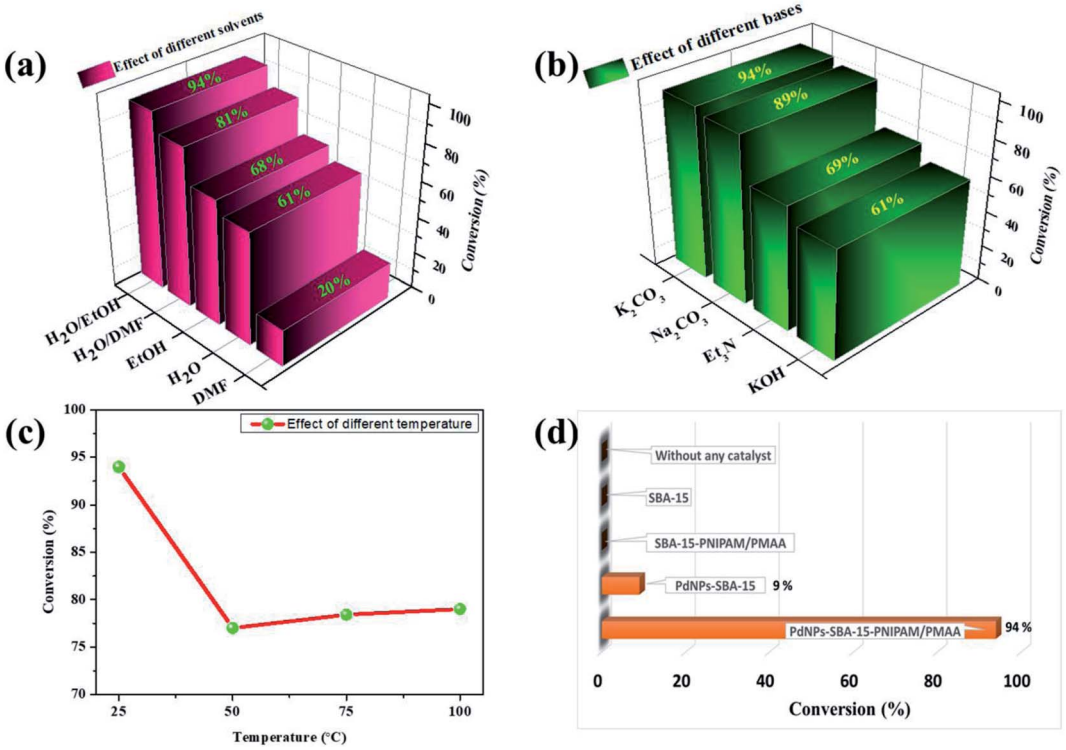

Fig. 9 (a) Effect of different solvents, (b) effect of different bases, (c) effect of temperature, and (d) results of controlled experiments on the SMC reaction between bromobenzene and phenylboronic acid. Reaction conditions: aryl halide = 1 mmol, phenylboronic acid = 1.3 mmol, TBAB = 0.5 mmol, base = 3 mmol, catalyst = 3 mg, and solvent = 5 mL. The conversion was determined by GC.

acid in an aqueous medium in the presence of TBAB at room temperature was investigated. Most coupling reactions are conducted using organic solvents at high temperatures. Thus, developing a new protocol for these reactions that could work at room temperatures in an aqueous medium should be challenging.

Significantly, to understand the role of the supporting material and to optimise the reaction conditions, we have explored the effects of variable parameters, such as solvents, bases, and temperatures. To find suitable solvents, we used dimethylformamide (DMF), ethanol, water, and their mixtures, and found that the ethanol–water (1 : 4) mixture was the most promising (Fig. 9a). Wei *et al.* reported 99% conversion for an SMC reaction using a DMF–water mixture at 90 °C.[35] In this study, we optimised the reaction using the ethanol–water mixture which is considered a green solvent with excellent conversion (94%) and selectivity (100%). Using the solvent mixture, ethanol enhances the solubility of organic moieties and water enables the swelling nature of catalyst collectively, leading to a good conversion among the individual solvents.

The base is an essential element for the activation of aryl halide and phenylboronic acid in coupling reactions. Thus, we inspected different bases, such as K_2CO_3, Na_2CO_3, KOH, and NEt_3, and observed that K_2CO_3 showed higher activity than the other bases and resulted in a good conversion of 94% (Fig. 9b). The relatively low activity of the organic base NEt_3 and inorganic base KOH could be attributed to the excess alkalinity, which results in homo-coupling of phenylboronic acid in water.[36] The order of the bases for the reactivity between bromobenzene and phenylboronic acid was K_2CO_3 > Na_2CO_3 > NEt_3 > KOH. The optimised catalyst amount was found to be 3 mg. When the catalyst amount increases, there is no significant difference in the rate of the reaction (Fig. S2†).

Next, impact of temperature on the SMC reaction was examined (Fig. 9c). As discussed, at 25 °C (below LCST), the conversion was found to be effective and reached 94%, whereas, at 50 °C (above LCST), the conversion decreased from 94% to 77%. As anticipated by the law of Arrhenius, the rate of the reaction is directly proportional to the temperature.[37] However, the activity of the catalyst was reduced further, and when the temperature was increased, there was an improvement in the catalytic activity towards the LCST behaviour of the PNIPAM moiety bound to the catalyst. During the reaction, below the LCST, the organic polymer on the catalyst exists in a swollen state; in this state, the reactant molecules can easily penetrate through the polymers and get adsorbed on the PdNP active sites

Table 2 SMC reactions of various aryl halides with phenylboronic acid over the PdNPs-SBA-15-PNIPAM/PMAA catalyst[a]

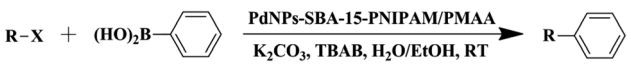

Entry	R–X	Product	Time (h)	Conversion (%)	Selectivity (%)	Isolated yield (%)
1		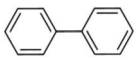	3	96	99	88
2	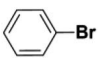	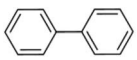	3	94	99	83
3		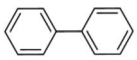	9	25	99	19
4	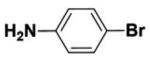	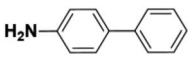	6	43	93	31
5	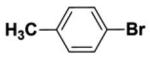	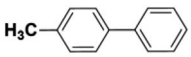	6	69	88	47
6	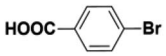	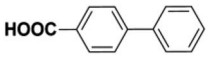	3	94	95	80
7	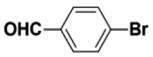	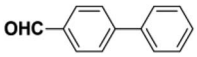	3	92	98	84
8	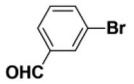	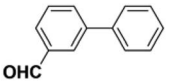	3	80	96	69
9	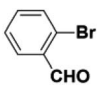	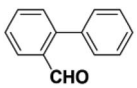	9	52	97	45

[a] Reaction conditions: Aryl halide = 1 mmol, phenylboronic acid = 1.3 mmol, TBAB = 0.5 mmol, K_2CO_3 = 3 mmol, catalyst = 3 mg, solvent = 5 ml H_2O/EtOH (4 : 1). Conversion and selectivity were determined by GC.

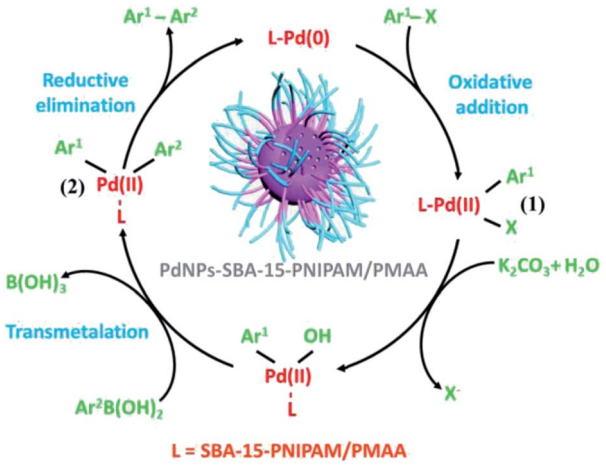

Scheme 3 The proposed mechanism for the SMC reaction.

that are incorporated in the mesopore. Meanwhile, above LCST, the catalyst gradually shrinks by ejecting the water molecule, which leads to a collapsed state of the polymer that restricts the reactants from interacting with the active site. As the reaction temperature was increased further from 50 °C through 75 °C to 100 °C, the catalyst collapsed completely, and the rate of conversion was not very effective on the catalytic pathway. Since we used K_2CO_3, the pH of the reacting system was around 10, and the PMAA moiety in the catalyst existed in the fully extended state because of the deprotonation of the COOH group. The synergetic effect of both temperature and pH leads to the relatively high activity of the catalyst at room temperature.

After optimising the base, temperature, and solvent, we performed controlled experiments to reveal the effect of the active site and the supporting material in the catalyst. Initially, we carried out the reaction in the absence of the catalyst and found that no expected products were formed. Additionally, replacing PdNPs-SBA-15-PNIPAM/PMAA with a PTC (TBAB) during the reaction showed no conversion, and the rate of conversion improved to 94% in the presence of both TBAB and the catalyst, whereas in the absence of TBAB, the conversion was 72%. The SBA-15, PdNPs-SBA-15, SBA-15-PNIPAM/PMAA, and PdNPs-SBA-15-PNIPAM/PMAA catalysts showed conversions of 0%, 9%, 0%, and 94%, respectively, in the presence of TBAB at room temperature (Fig. 9d). The PTC plays a vital role during coupling, and it increases the dissolution of the organic scaffolds in the aqueous medium.[38] In addition, TBAB anchored the PdNPs in the solution, prevented them from leaching, and caused maximum interaction between the substrate and PdNPs.[39]

Inspired from the above results, the catalyst was used to develop various substituted coupled products. To study the electronic and steric effects, a variety of aryl halides and phenylboronic acid were reacted in the presence of K_2CO_3 as a base and in an ethanol–water medium at room temperature. As illustrated in Table 2, among the aryl halides, bromobenzene and iodobenzene exhibited kinetically higher activity than chlorobenzene because the high electronegativity difference between carbon and halides restricts C–Cl bond cleavage in the order R–I > R–Br > R–Cl (Table 2, entries 1–3).[40] On comparing the electronic effect between the electron-releasing and electron-withdrawing groups, electron-rich 4-bromoaniline and 4-bromotoluene gave poor conversions compared to electron-deficient 4-bromobenzoic acid and 4-bromobenzaldehyde (Table 2, entries 4–7).[41] In the experiments conducted to understand the steric effect exerted by different electron-withdrawing groups, *p*-bromobenzaldehyde was consumed exceptionally well and gave excellent conversion compared to *m*-bromo and *o*-bromobenzaldehyde (Table 2, entries 7–9).[42]

To study the mechanistic pathway, the combined effect of SBA-15, PdNPs, and the stimuli-responsive polymers is

Table 3 Comparison of the catalytic activity of the PdNPs-SBA-15-PNIPAM/PMAA catalyst with that of the previously reported catalysts for SMC reactions[a]

Entry	Catalyst	Temperature (°C)	Time (h)	Yield (%)	Ref.
1	D-2PA-Pd(II)@SBA-15	120	5	85	44
2	Pd-diimine@SBA-15	80	12	87	45
3	Pd@SBA-15/IL_{DABCO}	80	12	95	46
4	Pd^0/SBA-15	110	4	80.2	47
5	SBA-15/di-urea/Pd	70	1	98	36
6	Pd-PS-*co*-PAEMA-*co*-PMAA	90 (H_2O)	6	99	48
7	Pd-PNIPAM-GPs	RT	24	96	49
8	**PdNPs-SBA-15-PNIPAM/PMAA**	**RT (H_2O/EtOH)**	**3**	**94**	**This work**

[a] RT: room temperature, D-2PA-Pd(II)@SBA-15: cycloaddition reaction between azido-functionalized mesoporous SBA-15 and *N*,*N*-dimethyl-2-propynylamine (D-2PA) followed by the complexation with $PdCl_2$, Pd-diimine@SBA-15: Immobilizing Pd onto diimine-functionalized mesoporous silica SBA-15, Pd@SBA-15/IL_{DABCO}: functionalization of SBA-15 with double-charged DABCO with 3-chloropropyltrimethoxysilane (CPTMS) and incorporated with Pd, Pd^0/SBA-15: palladium (Pd) nanoparticles were synthesized using the dendrimer-template method and then immobilized on a silica support (SBA-15), SBA-15/di-urea/Pd: palladium ions were anchored within the multidentate SBA-15/di-urea, Pd-PS-*co*-PAEMA-*co*-PMAA: Pd nanoparticles loaded into the pH-responsive colloid of core–shell microspheres of poly[styrene-*co*-2-(acetoacetoxy)ethyl methacrylate-*co*-methyl acrylic acid] (PS-*co*-PAEMA-*co*-PMAA), Pd-PNIPAM-GPs: PdNPs incorporated poly(*N*-isopropylacrylamide)-based hydrogel particles (GPs).

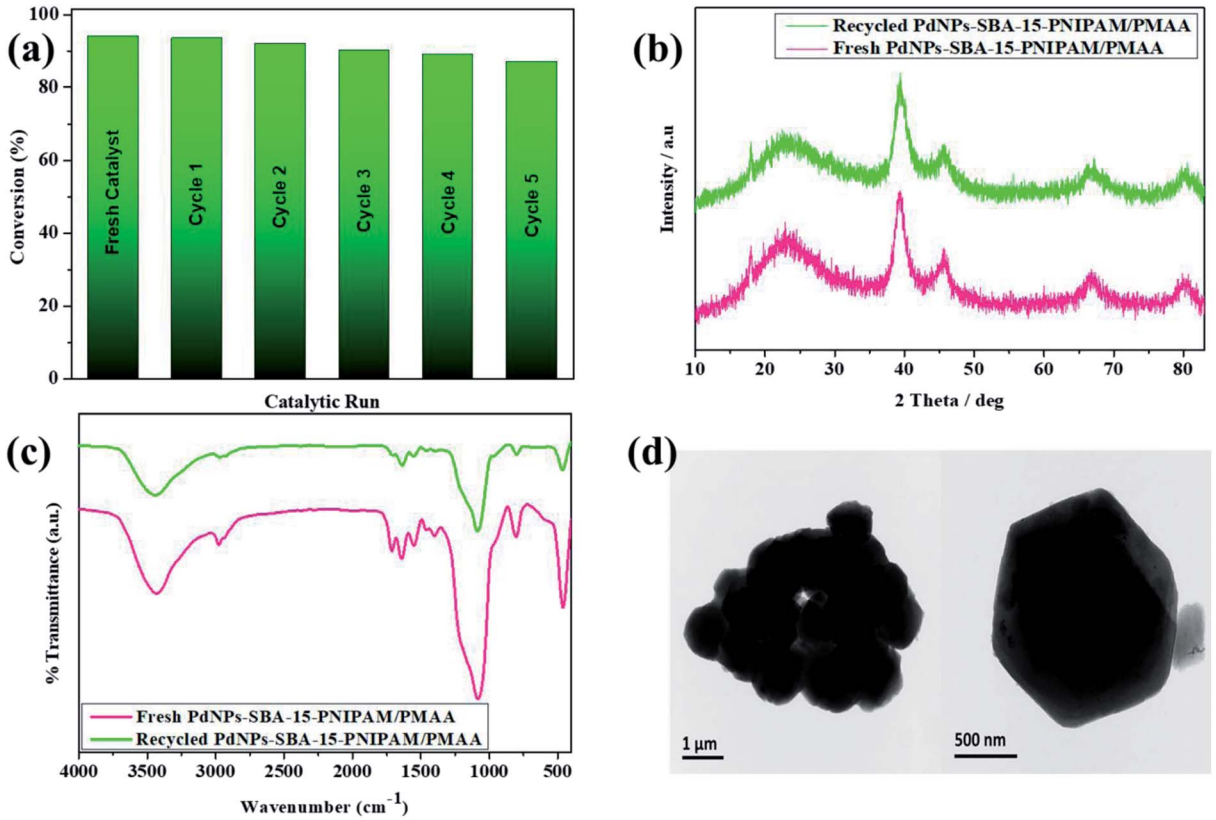

Fig. 10 (a) Reusability study of the PdNPs-SBA-15-PNIPAM/PMAA catalyst, (b) wide-angle XRD patterns, (c) FTIR spectra, and (d) FE-TEM images of the PdNPs-SBA-15-PNIPAM/PMAA catalyst after the fifth cycle. Reaction conditions: bromobenzene = 1 mmol, phenylboronic acid = 1.3 mmol, TBAB = 0.5 mmol, K_2CO_3 = 3 mmol, catalyst = 3 mg, solvent = water–ethanol (4 : 1). The conversion was determined by GC.

explained by a plausible route, demonstrated in Scheme 3, based on the above results and from the literature reports.[36,43] This route consists of three steps: oxidative addition, transmetalation, and reductive elimination. Initially, the oxidative addition of aryl halide to the Pd(0) complex to form an intermediate product **1** in Pd(II) state. Next, under basic conditions, transmetalation of the boronic acid compound produces intermediate **2**. Finally, the reductive elimination of intermediate **2** produces the final product, and the PdNPs were again regenerated into the active Pd(0) state. Table 3 presents the comparative study of our synthesised PdNPs-SBA-15-PNIPAM/PMAA with other previously reported Pd-supported catalysts for the coupling of aryl halides with phenylboronic acid.[36,44–49] Clearly, the catalyst reported herein showed comparable or better catalytic activity than other reported catalysts in terms of mild reaction conditions and green approaches.

Reusability of the catalyst

Another essential ability to consider for the heterogeneous catalyst is the recyclability of the catalyst. Owing to the economic and environmental factors, easy separation is crucial for the industrial process to reduce waste discharge and facilitate recyclability. In this study, the catalyst was separated by simple centrifugation, and recycling studies were performed for the reaction between bromobenzene and phenylboronic acid in a 4 : 1 water–ethanol mixture at room temperature. The PdNPs-SBA-15-PNIPAM/PMAA catalyst retained its catalytic activity over the five cycles (Fig. 10a). The reused catalyst was analysed by wide-angle XRD after the fifth cycle, and it revealed that the catalyst completely maintains its structural integrity (Fig. 10b). FTIR analysis confirmed the chemical integrity of the catalyst by comparing it with the fresh catalyst (Fig. 10c). To realise the stability of the catalyst, the FE-TEM (Fig. 10d) and TEM–EDX (Fig. S3†) analyses were performed after using the catalyst five consecutive times. The EDX data showed that less than 0.08% of PdNPs was leached out after the fifth wash. These results illustrate the excellent stability and robustness of the catalyst, which can be used multiple times in catalytic conversions.

Conclusions

In summary, a new heterogeneous PdNP-supportive smart hybrid catalyst with dual-responsive behaviour was prepared, and its responsiveness towards temperature and pH was characterised by DLS. The synthesised catalyst exhibited maximum swelling behaviour at relatively low temperatures and relatively high pH. Accordingly, the catalyst showed high catalytic efficiency and durability for the SMC reaction of less activated aryl halides at room temperature in an aqueous medium. The synergetic effect of the dual-responsive polymers and PdNPs enhanced the catalytic activity and allowed the reaction to

proceed under mild conditions. The catalyst was separated by simple centrifugation and reused five times without losing its catalytic activity and stability. The enhanced stability and robustness of our catalyst with the use of a less toxic solvent at room temperature suggest green and environment-friendly applications of our catalyst. Moreover, the obtained results also suggest that the simple tuning of pristine SBA-15 with dual-responsive polymers and PdNPs can form an outstanding material for the catalytic conversion in the SMC reaction. The temperature-responsive effect on the coupling reaction revealed that this system could be used as a temperature-programmable heterogeneous catalyst.

Conflicts of interest

There are no conflicts to declare.

Acknowledgements

The work was supported by National Research Foundation of Korea funded by Ministry of Science and ICT, Korea (NRF-2017R1A2B3012961); Brain Korea 21 Plus Program (21A2013800002).

Notes and references

1 J. Hassan, M. Sevignon, C. Gozzi, E. Schulz and M. Lemaire, Aryl-Aryl Bond Formation One Century after the Discovery of the Ullmann Reaction, *Chem. Rev.*, 2002, **102**, 1359–1470.
2 R. Hudson and J. L. Katz, Toward the Selection of Sustainable Catalysts for Suzuki–Miyaura Coupling: A Gate-to-Gate Analysis, *ACS Sustainable Chem. Eng.*, 2018, **6**(11), 14880–14887.
3 R. B. Bedford, M. E. Blake, C. P. Butt and D. Holder, The Suzuki coupling of aryl chlorides in TBAB-water mixture, *Chem. Commun.*, 2003, 466–467.
4 N. Kim, M. S. Kwon, C. M. Park and J. Park, One-pot synthesis of recyclable palladium catalysts for hydrogenations and carbon–carbon coupling reactions, *Tetrahedron Lett.*, 2004, **45**, 7057–7059.
5 I. Hoffmann, B. Blumenroder, S. O. Thumann, S. Dommer and J. Schatz, Suzuki cross-coupling un aqueous media, *Green Chem.*, 2015, **17**, 3844–3857.
6 W. A. Herrmann, N-Heterocyclic Carbenes: A New Concept in Organometallic Catalysis, *Angew. Chem., Int. Ed.*, 2002, **41**, 1290–1309.
7 K. Arentsen, S. Caddick, F. G. N. Cloke, A. P. Herring and P. B. Hitchcock, Suzuki–Miyaura cross-coupling of aryl and alkyl halides using palladium/imidazolium salt protocols, *Tetrahedron Lett.*, 2004, **45**, 3511–3515.
8 A. Mukherjee and A. Sarkar, New pyrazole-tethered Schiffs bases as ligands for the Suzuki reaction, *Tetrahedron Lett.*, 2005, **46**, 15–18.
9 N. Miyaura, T. Yanagigand and A. Suzuki, The Palladium-Catalyzed Cross-Coupling Reaction of Phenylboronic Acid with Haloarenes in the Presence of Bases, *Synth. Commun.*, 1981, **11**, 513–519.
10 I. P. Beletskaya and A. V. Cheprakov, The Heck Reaction as a Sharpening Stone of Palladium Catalysis, *Chem. Rev.*, 2000, **100**, 3009–3066.
11 I. Hussain, J. Capricho and M. A. Yawer, Synthesis of Biaryls via Ligand-Free Suzuki–Miyaura Cross-Coupling Reactions: A Review of Homogeneous and Heterogeneous Catalytic Developments, *Adv. Synth. Catal.*, 2016, **358**, 3320–3349.
12 A. Roucoux, J. Schulz and H. Patin, Reduced Transition Metal Colloids: A Novel Family of Reusable Catalysts?, *Chem. Rev.*, 2002, **102**, 3757–3778.
13 J. S. Chen, A. N. Vasiliev, A. P. Panarello and J. G. Khinast, Pd-leaching and Pd-removal in Pd/C-catalyzed Suzuki couplings, *Appl. Catal., A*, 2007, **325**, 76–86.
14 K. Kohler, R. G. Heidenreich, J. G. E. Krauter and J. Pietsch, Highly Active Palladium/Activated Carbon Catalysts for Heck Reactions: Correlation of Activity, Catalyst Properties, and Pd Leaching, *Chem. – Eur. J.*, 2002, **8**, 622–631.
15 G. M. Ziarani, S. Rohani, A. Ziarati and A. Badiei, Applications of SBA-15 supported Pd metal catalysts as nanoreactors in C–C coupling reactions, *RSC Adv.*, 2018, **8**, 41048–41100.
16 Z. Zheng, H. Li, T. Liu and R. Cao, Monodisperse noble metal nanoparticles stabilized in SBA-15: Synthesis, characterization and application in microwave-assisted Suzuki–Miyaura coupling reaction, *J. Catal.*, 2010, **270**, 268–274.
17 Y. Jiang and Q. Gao, Heterogeneous Hydrogenation Catalyses over Recyclable Pd(0) Nanoparticle Catalysts Stabilized by PAMAM-SBA-15 Organic–Inorganic Hybrid Composites, *J. Am. Chem. Soc.*, 2006, **128**, 716–717.
18 M. Bathfield, J. Reboul, T. Cacciaguerra, P. L. Desmazes and C. Gerardin, Thermosensitive and Drug-Loaded Ordered Mesoporous Silica: A Direct and Effective Synthesis Using PEO-b-PNIPAM Block Copolymers, *Chem. Mater.*, 2016, **28**, 3374–3384.
19 F. Liu and M. W. Urban, Recent advances and challenges in designing stimuli-responsive polymers, *Prog. Polym. Sci.*, 2010, **35**, 3–23.
20 Y. Yang, X. Ding and M. W. Urban, Chemical and physical aspects of self-healing materials, *Prog. Polym. Sci.*, 2015, **49**, 34–59.
21 Y. Zheng, L. Wang, L. Lu, Q. Wang and B. C. Benicewicz, pH and Thermal Dual-Responsive Nanoparticles for Controlled Drug Delivery with High Loading Content, *ACS Omega*, 2017, **2**(7), 3399–3405.
22 B. M. Cash, L. Wang and B. C. Benicewicz, The preparation and characterization of carboxylic acid-coated silica nanoparticles, *J. Polym. Sci., Part A: Polym. Chem.*, 2012, **50**, 2533–2540.
23 D. Schmaljohann, Thermo- And pH-responsive Polymers in Drug Delivery, *Adv. Drug Delivery Rev.*, 2006, **58**, 1655–1670.
24 D. Wang, Y. Jin, X. Zhu and D. Yan, Synthesis and applications of stimuli-responsive hyperbranched polymers, *Prog. Polym. Sci.*, 2017, **64**, 114–153.
25 L. Rout, A. Mohan, A. M. Thomas and C. S. Ha, Rational design of thermoresponsive functionalized MCM-41 and their decoration with bimetallic Ag–Pd nanoparticles for

catalytic application, *Microporous Mesoporous Mater.*, 2020, **291**, 109711–109721.

26 A. Mohan, L. Rout, A. M. Thomas, S. Nagappan, S. Parambadath, S. S. Park and C. S. Ha, Silver nanoparticles impregnated pH-responsive nanohybrid system for the catalytic reduction of dyes, *Microporous Mesoporous Mater.*, 2020, **303**, 110260–110269.

27 F. Azimov, I. Markova, V. Stefanova and K. H. Sharipov, Synthesis and Characterization of SBA-15 and Ti-SBA-15 Nanoporous Materials for DME catalysts, *J. Chem. Technol. Metall.*, 2012, **47**, 333–340.

28 R. Nechikkattu and C. S. Ha, Tunable catalytic activity of gold nanoparticle decorated SBA-15/PDMAEMA hybrid system, *J. Porous Mater.*, 2020, **27**, 611–620.

29 S. Nagappan, S. S. Park, B. K. Kim, D. Yoo, N. Jo, W. K. Lee and C. S. Ha, Synthesis and functionalisation of mesoporous materials for transparent coatings and organic dye adsorption, *New J. Chem.*, 2018, **42**, 10254–10262.

30 A. M. Thomas, A. Mohan, L. Rout, S. Nagappan, S. S. Park and C. S Ha, Pd nanoparticle incorporated mesoporous silicas with excellent catalytic activity and dual responsivity, *Colloids Surf., A*, 2020, **585**, 124074–124084.

31 V. A. Valles, Y. Sa- ngasaeng, M. L. Martínez, S. Jongpatiwut and A. R. Beltramone, HDT of the model diesel feed over Ir-modified Zr-SBA-15 catalysts, *Fuel*, 2019, **240**, 138–152.

32 Z. Gong, S. Li, J. Ma and X. Zhang, Synthesis of recyclable powdered activated carbon with temperature responsive polymer for bisphenol A removal, *Sep. Purif. Technol.*, 2016, **157**, 131–140.

33 R. Regmi, S. R. Bhattarai, C. Sudakar, A. S. Wani, R. Cunningham, P. P. Vaishnava, R. Naik, D. Oupicky and G. Lawes, Hyperthermia controlled rapid drug release from thermosensitive magnetic microgels, *J. Mater. Chem.*, 2010, **20**, 6158–6163.

34 S. Ashraf, R. Begum, R. Rehan, W. Wu and Z. H. Farooqi, Synthesis and Characterization of pH-Responsive Organic–Inorganic Hybrid Material with Excellent Catalytic Activity, *J. Inorg. Organomet. Polym. Mater.*, 2018, **28**, 1872–1884.

35 G. Wei, W. Zhang, F. Wen, Y. Wang and M. Zhang, Suzuki Reaction within the Core−Corona Nanoreactor of Poly(N-isopropylacrylamide)-Grafted Pd Nanoparticle in Water, *J. Phys. Chem. C*, 2008, **112**, 10827–10832.

36 S. Rohani, G. M. Ziarani, A. Badiei, A. Ziarati, M. Jafari and A. Shayesteh, Palladium-anchored multidentate SBA-15/di-urea nanoreactor: A highly active catalyst for Suzuki coupling reaction, *Appl. Organomet. Chem.*, 2018, **32**, e4397.

37 L. Tzounis, M. Dona, J. M. L. Romero, A. Fery and R. C. Caceres, Temperature-Controlled Catalysis by Core–Shell–Satellite AuAg@pNIPAM@Ag Hybrid Microgels: A Highly Efficient Catalytic Thermoresponsive Nanoreactor, *ACS Appl. Mater. Interfaces*, 2019, **11**, 29360–29372.

38 B. Li, C. Wang, G. Chen and Z. Zhang, Palladium-phosphinous acid complexes catalyzed Suzuki cross-coupling reaction of heteroaryl bromides with phenylboronic acid in water/alcoholic solvents, *J. Environ. Sci.*, 2013, **25**, 1083–1088.

39 S. S. Soomro, C. Rohlich and K. Kohler, Suzuki Coupling Reactions in Pure Water Catalyzed by Supported Palladium – Relevance of the Surface Polarity of the Support, *Adv. Synth. Catal.*, 2011, **353**, 767–775.

40 G. E. Davico, V. M. Bierbaum, C. H. Depuy, G. B. Ellison and R. R. Squires, The C-H Bond Energy of Benzene, *J. Am. Chem. Soc.*, 1995, **117**, 2590–2599.

41 P. Jerome, P. N. Sathishkumar, N. S. P. Bhuvanesh and R. Karvembu, Towards phosphine-free Pd(II) pincer complexes for catalyzing Suzuki-Miyaura cross-coupling reaction in aqueous medium, *J. Organomet. Chem.*, 2017, **845**, 115–124.

42 P. Jerome, S. Y. Arafath, J. Haribabu, N. S. P. Bhuvanesh and R. Karvembu, Effect of 2-Bromopyridine Ancillary Ligand in the Catalysis of Pd(II)-NNN Pincer Complexes towards Suzuki-Miyaura Cross-Coupling Reaction, *ChemistrySelect*, 2019, **4**, 2237–2241.

43 D. Ogawa, K. Hyodo, M. Suetsugu, J. Li, Y. Inoue, M. Fujisawa, M. Iwasaki, K. Takagi and Y. Nishihara, Palladium-catalyzed and copper-mediated cross-coupling reaction of aryl- or alkenylboronic acids with acid chlorides under neutral conditions: efficient synthetic methods for diaryl ketones and chalcones at room temperature, *Tetrahedron*, 2013, **69**, 2565–2571.

44 A. Pathak and A. P. Singh, Synthesis and characterization of D-2PA-Pd(II)@SBA-15 catalyst via "click chemistry": highly active catalyst for Suzuki coupling reactions, *J. Porous Mater.*, 2017, **24**, 327–340.

45 J. Yu, A. Shen, Y. Cao and G. Lu, Preparation of Pd-Diimine@SBA-15 and Its Catalytic Performance for the Suzuki Coupling Reaction, *Catalysts*, 2016, **6**, 181–198.

46 S. Rostamnia, E. Doustkhah and B. Zeynzadeh, Cationic modification of SBA-15 pore walls for Pd supporting: Pd@SBA-15/IL_{DABCO} as a catalyst for Suzuki coupling in water medium, *Microporous Mesoporous Mater.*, 2016, **222**, 87–93.

47 P. Ncube, T. Hlabathe and R. Meijboom, Palladium Nanoparticles Supported on Mesoporous Silica as Efficient and Recyclable Heterogenous Nanocatalysts for the Suzuki C–C Coupling Reaction, *J. Cluster Sci.*, 2015, **26**, 1873–1888.

48 P. Zheng and W. Zhang, Synthesis of efficient and reusable palladium catalyst supported on pH-responsive colloid and its application to Suzuki and Heck reactions in water, *J. Catal.*, 2007, **250**, 324–330.

49 H. Matsumoto, T. Akiyoshi, Y. Hoshino, H. Seto and Y. Miura, Size-tuned hydrogel network of palladium-confining polymer particles: a highly active and durable catalyst for Suzuki coupling reactions in water at ambient temperature, *Polym. J.*, 2018, **50**, 1179–1186.

